Computational Study on Novel $RhCp^X$ ($X = CF_3$, SiF_3, CCl_3, SO_3H) as Promising Catalysts in the [3+2] Azide–Alkyne Cycloaddition Reaction: Insights into Mechanistic Pathways and Reactivity

Ali A Khairbek[1,8], Mohammad Abd-Al Hakim Badawi[2], Abdullah Y. Alzahrani[3], Ralph Puchta[4,5,6] and Renjith Thomas[7,8]

[1] Centre of Molecular Medicine and Diagnostics (COMManD), Saveetha Dental College and Hospitals, Saveetha Institute of Medical and Technical Sciences, Saveetha University, Chennai 600 077, India
[2] Department of Chemistry, Faculty of Science, Tishreen University, Latakia, Syrian Arab Republic.
[3] Department of Chemistry, Faculty of Science and Arts, King Khalid University, Mohail Assir, Saudi Arabia;
[4] Inorganic Chemistry, Department of Chemistry and Pharmacy, University of Erlangen-Nuremberg, Erlangen, Germany
[5] Computer Chemistry Center, Department of Chemistry and Pharmacy, University of Erlangen-Nuremberg, Erlangen, Germany
[6] Central Institute for Scientific Computing (CISC), University of Erlangen-Nuremberg, Erlangen, Germany
[7] Department of Chemistry, St Berchmans College (Autonomous), Changanassery, Kerala, India-686101.
[8] Centre for Theoretical and Computational Chemistry, St Berchmans College (Autonomous), Changanassery, Kerala, India-686101.

Corresponding Authors:
Ali A Khairbek MRSC: alikhairbek@gmail.com
Renjith Thomas FRSC: renjith@sbcollege.ac.in

NCI and RDG Analysis

To gain a comprehensive understanding of the catalytic behavior of the $RhCp^X$ complexes, we first focus on the analysis of the Cp^X ligands themselves. Using Non-Covalent Interaction (NCI) and Reduced Density Gradient (RDG) analyses, we investigate the stability and interaction patterns of the Cp^X ligands, which play a key role in modulating the reactivity of the catalyst. These initial insights into the ligand interactions pave the way for a detailed mechanistic exploration of the [3+2] azide-alkyne cycloaddition reaction.

NCI and RDG analyses are powerful computational tools used to visualize and quantify weak interactions in molecular systems [35–38]. NCI provides a detailed map of noncovalent interactions such as hydrogen bonds, van der Waals forces, and repulsive steric effects by analyzing electron density regions. RDG complements this by identifying regions of low

electron density gradients, which correspond to noncovalent interactions, and characterizing them on the basis of their strength. Together, the NCI and RDG plots offer valuable insights into the stability and behavior of molecular complexes, aiding in the understanding of their molecular structures and reactivities. These methods are especially useful for studying weak interactions in both small molecules and complex systems.

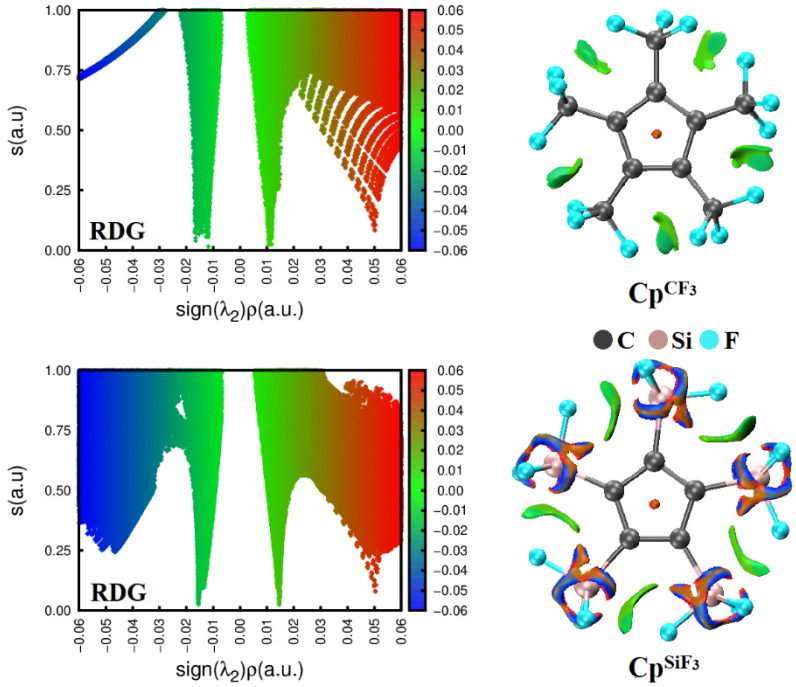

Figure S1. RDG and NCI plots for Cp^{CF_3} and Cp^{SiF_3}.

The RDG and NCI plots for the ligands Cp^{CF_3} and Cp^{SiF_3} were analyzed to assess their stability on the basis of their noncovalent interactions (Figure S1). The Cp^{CF_3} ligand demonstrated moderate stability, primarily due to the weak interactions observed around the fluorine atoms. The RDG plots reveal some red regions, which indicate weak repulsive interactions, limiting the overall stability of the ligand. Although van der Waals forces contribute to its structure, the absence of strong attractive forces reduces its effectiveness in more reactive or demanding environments. In contrast, the Cp^{SiF_3} ligand exhibited better stability. The RDG and NCI plots highlight strong attractive interactions between the fluorine and silicon atoms, evident from the blue and green regions, which signify favorable noncovalent attractions. These interactions strengthen the ligand's structure, ensuring more robust stability under various conditions. On the other hand, Cp^{CCl_3} relies heavily on weak van der Waals forces, as indicated by the peaks near zero in the RDG plots in Figure S2. These weak interactions around the chlorine atoms suggest limited stability, as the ligand lacks significant attractive forces to hold its structure firmly in place. The absence of blue or green regions in the NCI plots further supports the conclusion that Cp^{CCl_3} has reduced stability compared with other ligands. Finally, Cp^{SO_3H} displays the highest stability among the four ligands. The RDG plots show distinct blue and green regions, indicating strong hydrogen bonding between the oxygen and sulfur atoms. These attractive interactions provide a solid foundation for the ligand's structure, making it the most stable in terms of noncovalent interactions.

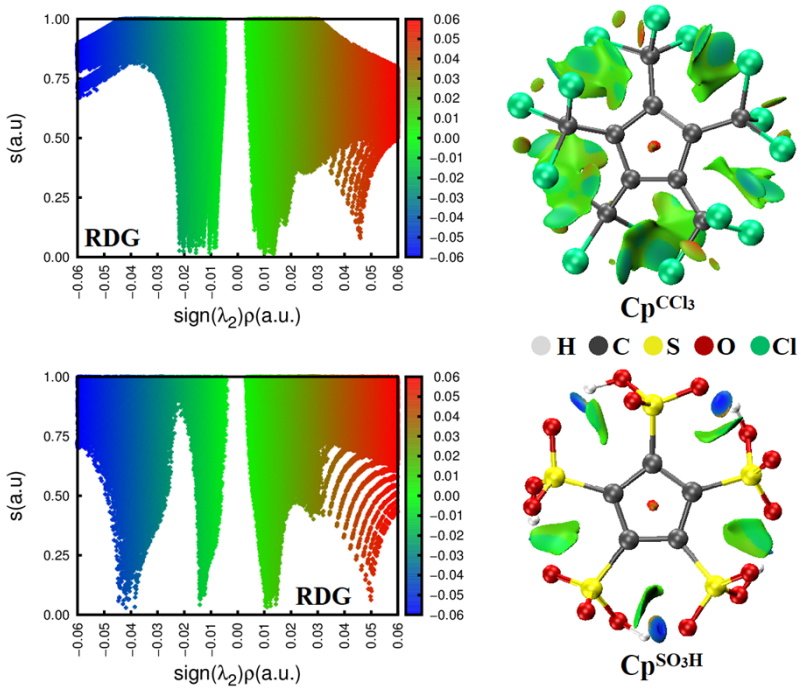

Figure S2. RDG and NCI plots for Cp^{CCl_3} and Cp^{SO_3H}.

Cp^{CF_3} and Cp^{CCl_3} demonstrate moderate to weak stability because of their reliance on weak interactions. Cp^{SiF_3} and Cp^{SO_3H} show greater stability because of the strong noncovalent attractions that enhance their molecular structure.

Table S1: ΔG_{298} (kcal/mol) in the gas phase and solvents for the Cp^{CF_3} in 1-4 pathways.

	Cp^{CF_3}						
ΔG_{298}	gas phase	Toluene	THF	Cyclohexane	benzene	Acetonitrile	water
$RC_{1\text{-}4}$	-4.4	-3.0	-2.3	-3.2	-3.0	-2.0	-2.0
$TS1_{1\text{-}4}$	11.0	12.2	12.8	12.0	12.2	13.1	13.1
$IC_{1\text{-}4}$	-26.2	-25.3	-25.0	-25.4	-25.4	-24.9	-24.9
$TS2_{1\text{-}4}$	9.8	10.3	10.5	10.3	10.3	10.5	10.5
$P_{1\text{-}4}$	-52.6	-53.3	-53.8	-53.1	-53.2	-54.1	-54.2

Table S2: ΔG_{298} (kcal/mol) in the gas phase and solvents for the Cp^{SiF_3} in 1-4 pathways.

	Cp^{SiF_3}						
ΔG_{298}	gas phase	Toluene	THF	Cyclohexane	benzene	Acetonitrile	water
$RC_{1\text{-}4}$	-4.6	-2.5	-1.4	-2.8	-2.6	-1.0	-1.0
$TS1_{1\text{-}4}$	12.6	14.4	15.2	14.1	14.3	15.6	15.6
$IC_{1\text{-}4}$	-25.4	-24.1	-23.6	-24.3	-24.2	-23.5	-23.5
$TS2_{1\text{-}4}$	8.5	9.8	10.4	9.7	9.8	10.5	10.6
$P_{1\text{-}4}$	-55.8	-55.5	-55.5	-55.5	-55.5	-55.5	-55.5

Table S3: ΔG_{298} (kcal/mol) in the gas phase and solvents for the Cp^{CCl_3} in 1-4 pathways.

	Cp^{CCl_3}						
ΔG_{298}	gas phase	Toluene	THF	Cyclohexane	benzene	Acetonitrile	water
RC_{1-4}	2.4	3.1	3.4	3.0	3.1	3.5	3.5
$TS1_{1-4}$	16.3	17.5	18.2	17.4	17.5	18.4	18.5
IC_{1-4}	-24.7	-23.9	-23.5	-24.0	-23.9	-23.4	-23.4
$TS2_{1-4}$	11.7	12.0	12.0	12.0	12.0	12.0	12.0
P_{1-4}	-45.9	-47.6	-48.8	-47.3	-47.5	-49.3	-49.4

Table S4: ΔG_{298} (kcal/mol) in the gas phase and solvents for the Cp^{SO_3H} in 1-4 pathways.

	Cp^{SO_3H}						
ΔG_{298}	gas phase	Toluene	THF	Cyclohexane	benzene	Acetonitrile	water
RC_{1-4}	-7.9	-5.0	-3.3	-5.4	-5.1	-2.7	-2.6
$TS1_{1-4}$	5.1	8.3	10.0	7.8	8.1	10.7	10.8
IC_{1-4}	-28.7	-26.3	-25.1	-26.6	-26.4	-24.6	-24.6
$TS2_{1-4}$	-6.6	-4.4	-3.3	-4.7	-4.5	-2.9	-2.9
P_{1-4}	-59.6	-60.2	-60.6	-60.1	-60.2	-60.7	-60.7

Table S5: ΔG_{298} (kcal/mol) in the gas phase and solvents for the Cp^{CF_3} in 1-5 pathways.

	Cp^{CF_3}						
ΔG_{298}	gas phase	Toluene	THF	Cyclohexane	benzene	Acetonitrile	water
RC_{1-5}	-5.4	-3.8	-2.9	-4.0	-3.8	-2.6	-2.6
$TS1_{1-5}$	7.6	9.3	10.2	9.0	9.2	10.5	10.6
IC_{1-5}	-8.0	-7.8	-7.9	-7.8	-7.8	-7.9	-7.9
$TS2_{1-5}$	-3.6	-3.2	-3.1	-3.2	-3.2	-3.1	-3.1
P_{1-5}	-29.0	-36.3	-41.1	-35.2	-36.0	-43.3	-43.6

Table S6: ΔG_{298} (kcal/mol) in the gas phase and solvents for the Cp^{SiF_3} in 1-5 pathways.

	Cp^{SiF_3}						
ΔG_{298}	gas phase	Toluene	THF	Cyclohexane	benzene	Acetonitrile	water
RC_{1-5}	-5.1	-2.8	-1.6	-3.1	-2.9	-1.1	-1.1
$TS1_{1-5}$	4.5	7.0	8.3	6.6	6.9	8.8	8.9
IC_{1-5}	-7.4	-6.9	-6.7	-6.9	-6.9	-6.7	-6.7
$TS2_{1-5}$	-2.2	-1.7	-1.7	-1.8	-1.7	-1.7	-1.7
P_{1-5}	-34.4	-37.9	-40.3	-37.4	-37.8	-41.3	-41.5

Table S7: ΔG_{298} (kcal/mol) in the gas phase and solvents for the Cp^{CCl_3} in 1-5 pathways.

	Cp^{CCl_3}						
ΔG_{298}	gas phase	Toluene	THF	Cyclohexane	benzene	Acetonitrile	water
RC_{1-5}	5.6	6.3	6.5	6.2	6.2	6.6	6.7
$TS1_{1-5}$	11.8	12.9	13.5	12.7	12.8	13.7	13.7
IC_{1-5}	-2.4	-3.2	-3.9	-3.1	-3.2	-4.2	-4.2
$TS2_{1-5}$	2.5	2.4	2.3	2.4	2.4	2.2	2.2
P_{1-5}	-58.5	-62.6	-65.4	-62.0	-62.5	-66.6	-66.8

Table S8: ΔG_{298} (kcal/mol) in the gas phase and solvents for the Cp^{SO_3H} in 1-5 pathways.

	Cp^{SO_3H}						
ΔG_{298}	gas phase	Toluene	THF	Cyclohexane	benzene	Acetonitrile	water
RC_{1-5}	-9.2	-6.9	-5.7	-7.2	-7.0	-5.2	-5.2
$TS1_{1-5}$	0.2	3.3	4.9	2.8	3.1	5.6	5.7
IC_{1-5}	-14.7	-13.0	-12.2	-13.2	-13.1	-12.0	-11.9
$TS2_{1-5}$	-7.2	-5.7	-5.1	-5.9	-5.8	-4.9	-4.9
P_{1-5}	-49.0	-56.8	-62.0	-55.6	-56.5	-64.3	-64.6

Table S9. G_{corr} in the gas phase and (E_o) in the solvent (in Hartree) of catalytic cycle components with Cp^{CF_3}, for 1,4 RhAAC reaction pathways.

	Cp^{CF_3}			
	Go_{GAS}	Eo_{GAS}	$Eo_{Toluene}$	Eo_{THF}
AC	0.162202	-2293.726625	-2293.731588	-2293.734230
RC_{1-4}	0.286952	-2728.151960	-2728.157989	-2728.161277
$TS1_{1-4}$	0.287372	-2728.127977	-2728.134194	-2728.137589
IC_{1-4}	0.294852	-2728.194676	-2728.201504	-2728.205328
$TS2_{1-4}$	0.291947	-2728.134426	-2728.141787	-2728.145940
P_{1-4}	0.293015	-2728.234925	-2728.244147	-2728.249470
	$Eo_{Cyclohexane}$	$Eo_{benzene}$	$Eo_{Acetonitrile}$	Eo_{Water}
AC	-2293.730920	-2293.731415	-2293.731415	-2293.735397
RC_{1-4}	-2728.157168	-2728.157777	-2728.157777	-2728.162749
$TS1_{1-4}$	-2728.133347	-2728.133975	-2728.133975	-2728.139111
IC_{1-4}	-2728.200562	-2728.201260	-2728.201260	-2728.207074
$TS2_{1-4}$	-2728.140767	-2728.141523	-2728.141523	-2728.147841
P_{1-4}	-2728.242853	-2728.243811	-2728.243811	-2728.251938

Table S10. G_{corr} in the gas phase and (E_o) in the solvent (in Hartree) of catalytic cycle components with Cp^{SiF_3}, for 1,4 RhAAC reaction pathways.

	Cp^{SiF_3}			
	Go_{GAS}	Eo_{GAS}	$Eo_{Toluene}$	Eo_{THF}
AC	0.128667	-3551.269209	-3551.279065	-3551.284276
RC_{1-4}	0.252740	-3985.694194	-3985.704002	-3985.709261
$TS1_{1-4}$	0.257379	-3985.671463	-3985.681775	-3985.687339
IC_{1-4}	0.262193	-3985.736853	-3985.747931	-3985.754081
$TS2_{1-4}$	0.259030	-3985.679618	-3985.690665	-3985.696768
P_{1-4}	0.260945	-3985.784047	-3985.796637	-3985.803560
	$Eo_{Cyclohexane}$	$Eo_{benzene}$	$Eo_{Acetonitrile}$	Eo_{Water}
AC	-3551.277745	-3551.278724	-3551.278724	-3551.286570
RC_{1-4}	-3985.702679	-3985.703660	-3985.703660	-3985.711595
$TS1_{1-4}$	-3985.680379	-3985.681414	-3985.681414	-3985.689821
IC_{1-4}	-3985.746410	-3985.747537	-3985.747537	-3985.756879
$TS2_{1-4}$	-3985.689152	-3985.690273	-3985.690273	-3985.699531
P_{1-4}	-3985.794917	-3985.796192	-3985.796192	-3985.806682

Table S11. G_{corr} in the gas phase and (E_o) in the solvent (in Hartree) of catalytic cycle components with Cp^{CCl_3}, for 1,4 RhAAC reaction pathways.

	Cp^{CCl_3}			
	Go_{GAS}	Eo_{GAS}	$Eo_{Toluene}$	Eo_{THF}
AC	0.123480	-7697.305251	-7697.309339	-7697.311523
RC_{1-4}	0.249982	-8131.721629	-8131.727808	-8131.731216
$TS1_{1-4}$	0.251884	-8131.701342	-8131.706671	-8131.709569
IC_{1-4}	0.254438	-8131.769266	-8131.775272	-8131.778630
$TS2_{1-4}$	0.256469	-8131.713194	-8131.720073	-8131.723951
P_{1-4}	0.257800	-8131.806366	-8131.816368	-8131.822224
	$Eo_{Cyclohexane}$	$Eo_{benzene}$	$Eo_{Acetonitrile}$	Eo_{Water}
AC	-7697.308789	-7697.309197	-7697.309197	-7697.312490
RC_{1-4}	-8131.726962	-8131.727589	-8131.727589	-8131.732754
$TS1_{1-4}$	-8131.705947	-8131.706484	-8131.706484	-8131.710865
IC_{1-4}	-8131.774445	-8131.775058	-8131.775058	-8131.780164
$TS2_{1-4}$	-8131.719120	-8131.719826	-8131.719826	-8131.725727
P_{1-4}	-8131.814956	-8131.816001	-8131.816001	-8131.824970

Table S12. G_{corr} in the gas phase and (E_o) in the solvent (in Hartree) of catalytic cycle components with Cp^{SO_3H}, for 1,4 RhAAC reaction pathways.

	Cp^{SO_3H}			
	Go GAS	*Eo* GAS	*Eo* Toluene	*Eo* THF
AC	0.214747	-3727.022047	-3727.037250	-3727.045527
RC_{1-4}	0.338453	-4161.451950	-4161.465765	-4161.473187
$TS1_{1-4}$	0.340499	-4161.433256	-4161.446725	-4161.453961
IC_{1-4}	0.346972	-4161.493601	-4161.508247	-4161.516329
$TS2_{1-4}$	0.348124	-4161.459567	-4161.474557	-4161.482838
P_{1-4}	0.343664	-4161.539561	-4161.558971	-4161.569588
	Eo Cyclohexane	*Eo* benzene	*Eo* Acetonitrile	*Eo* Water
AC	-3727.035184	-3727.036716	-3727.036716	-3727.049239
RC_{1-4}	-4161.463900	-4161.465283	-4161.465283	-4161.476489
$TS1_{1-4}$	-4161.444907	-4161.446255	-4161.446255	-4161.457182
IC_{1-4}	-4161.506245	-4161.507728	-4161.507728	-4161.520000
$TS2_{1-4}$	-4161.472506	-4161.474026	-4161.474026	-4161.486597
P_{1-4}	-4161.556325	-4161.558286	-4161.558286	-4161.574356

Table S13. G_{corr} in the gas phase and (E_o) in the solvent (in Hartree) of catalytic cycle components with Cp^{CF_3}, for 1,5 RhAAC reaction pathways.

	Cp^{CF_3}			
	Go GAS	*Eo* GAS	*Eo* Toluene	*Eo* THF
AC	0.162202	-2293.726625	-2293.731588	-2293.734230
RC_{1-5}	0.285427	-2728.152049	-2728.157710	-2728.160756
$TS1_{1-5}$	0.289855	-2728.135815	-2728.141342	-2728.144314
IC_{1-5}	0.290378	-2728.161159	-2728.169070	-2728.173578
$TS2_{1-5}$	0.291445	-2728.155267	-2728.162788	-2728.167032
P_{1-5}	0.292128	-2728.196413	-2728.216179	-2728.228352
	Eo Cyclohexane	*Eo* benzene	*Eo* Acetonitrile	*Eo* Water
AC	-2293.730920	-2293.731415	-2293.731415	-2293.735397
RC_{1-5}	-2728.156945	-2728.157512	-2728.157512	-2728.162110
$TS1_{1-5}$	-2728.140595	-2728.141149	-2728.141149	-2728.145634
IC_{1-5}	-2728.167968	-2728.168784	-2728.168784	-2728.175653
$TS2_{1-5}$	-2728.161746	-2728.162518	-2728.162518	-2728.168977
P_{1-5}	-2728.213315	-2728.215432	-2728.215432	-2728.234234

Table S14. G_{corr} in the gas phase and (E_o) in the solvent (in Hartree) of catalytic cycle components with Cp^{SiF_3}, for 1,4 RhAAC reaction pathways.

	Cp^{SiF_3}			
	Go_{GAS}	Eo_{GAS}	$Eo_{Toluene}$	Eo_{THF}
AC	0.128667	-3551.269209	-3551.279065	-3551.284276
RC_{1-5}	0.252959	-3985.695197	-3985.704691	-3985.709735
$TS1_{1-5}$	0.255171	-3985.682251	-3985.691356	-3985.696180
IC_{1-5}	0.258031	-3985.704090	-3985.716251	-3985.722989
$TS2_{1-5}$	0.257396	-3985.695121	-3985.707434	-3985.714330
P_{1-5}	0.260448	-3985.749444	-3985.768112	-3985.778860
	$Eo_{Cyclohexane}$	$Eo_{benzene}$	$Eo_{Acetonitrile}$	Eo_{Water}
AC	-3551.277745	-3551.278724	-3551.278724	-3551.286570
RC_{1-5}	-3985.703416	-3985.704362	-3985.704362	-3985.711962
$TS1_{1-5}$	-3985.690136	-3985.691041	-3985.691041	-3985.698306
IC_{1-5}	-3985.714583	-3985.715819	-3985.715819	-3985.726041
$TS2_{1-5}$	-3985.705736	-3985.706994	-3985.706994	-3985.717482
P_{1-5}	-3985.765502	-3985.767434	-3985.767434	-3985.783867

Table S15. G_{corr} in the gas phase and (E_o) in the solvent (in Hartree) of catalytic cycle components with Cp^{CCl_3}, for 1,5 RhAAC reaction pathways.

	Cp^{CCl_3}			
	Go_{GAS}	Eo_{GAS}	$Eo_{Toluene}$	Eo_{THF}
AC	0.123480	-7697.305251	-7697.309339	-7697.311523
RC_{1-5}	0.249411	-8131.715868	-8131.722189	-8131.725655
$TS1_{1-5}$	0.250528	-8131.707171	-8131.712731	-8131.715744
IC_{1-5}	0.253221	-8131.732422	-8131.741084	-8131.746045
$TS2_{1-5}$	0.255477	-8131.726957	-8131.734360	-8131.738542
P_{1-5}	0.253767	-8131.822376	-8131.836322	-8131.844650
	$Eo_{Cyclohexane}$	$Eo_{benzene}$	$Eo_{Acetonitrile}$	Eo_{Water}
AC	-7697.308789	-7697.309197	-7697.309197	-7697.312490
RC_{1-5}	-8131.721326	-8131.721966	-8131.721966	-8131.727215
$TS1_{1-5}$	-8131.711977	-8131.712536	-8131.712536	-8131.717088
IC_{1-5}	-8131.739875	-8131.740770	-8131.740770	-8131.748339
$TS2_{1-5}$	-8131.733335	-8131.734094	-8131.734094	-8131.740461
P_{1-5}	-8131.834335	-8131.835805	-8131.835805	-8131.848607

Table S16. G_{corr} in the gas phase and (E_o) in the solvent (in Hartree) of catalytic cycle components with Cp^{SO_3H}, for 1,5 RhAAC reaction pathways.

	Cp^{SO_3H}			
	Go GAS	*Eo* GAS	*Eo* Toluene	*Eo* THF
AC	0.214747	-3727.022047	-3727.037250	-3727.045527
RC_{1-5}	0.339582	-4161.455222	-4161.469979	-4161.478061
$TS1_{1-5}$	0.339190	-4161.439838	-4161.453385	-4161.460727
IC_{1-5}	0.341056	-4161.465382	-4161.481155	-4161.489943
$TS2_{1-5}$	0.344048	-4161.456414	-4161.472588	-4161.481635
P_{1-5}	0.346065	-4161.525034	-4161.556004	-4161.574344
	Eo Cyclohexane	*Eo* benzene	*Eo* Acetonitrile	*Eo* Water
AC	-3727.035184	-3727.036716	-3727.036716	-3727.049239
RC_{1-5}	-4161.467967	-4161.469458	-4161.469458	-4161.481698
$TS1_{1-5}$	-4161.451549	-4161.452911	-4161.452911	-4161.464017
IC_{1-5}	-4161.478987	-4161.480594	-4161.480594	-4161.493948
$TS2_{1-5}$	-4161.470359	-4161.472011	-4161.472011	-4161.485763
P_{1-5}	-4161.551605	-4161.554860	-4161.554860	-4161.582993

Atomic dipole-corrected Hirshfeld atomic charge (ADCH) for AC_RhCp^{CF_3}

```
Final atomic charges, after normalization to actual number of
electrons
 Atom    1(C ):    -0.13877608
 Atom    2(C ):    -0.83828690
 Atom    3(C ):    -0.10303835
 Atom    4(C ):     0.00864256
 Atom    5(C ):     0.02062892
 Atom    6(C ):     0.35980544
 Atom    7(C ):     0.40270287
 Atom    8(H ):     0.35051266
 Atom    9(Rh):    -0.37861630
 Atom   10(C ):     0.76779564
 Atom   11(C ):     0.85977128
 Atom   12(C ):     0.86199833
 Atom   13(C ):     0.85500632
 Atom   14(C ):     0.85881148
 Atom   15(C ):     0.00134304
 Atom   16(C ):    -0.00445944
 Atom   17(C ):    -0.08382596
 Atom   18(C ):    -0.11655235
 Atom   19(C ):    -0.13428521
 Atom   20(C ):    -0.11443192
 Atom   21(H ):     0.08995164
 Atom   22(H ):     0.12809188
 Atom   23(H ):     0.12761050
 Atom   24(H ):     0.12494102
 Atom   25(H ):     0.12868419
 Atom   26(F ):    -0.25740598
 Atom   27(F ):    -0.25967537
 Atom   28(F ):    -0.29078029
```

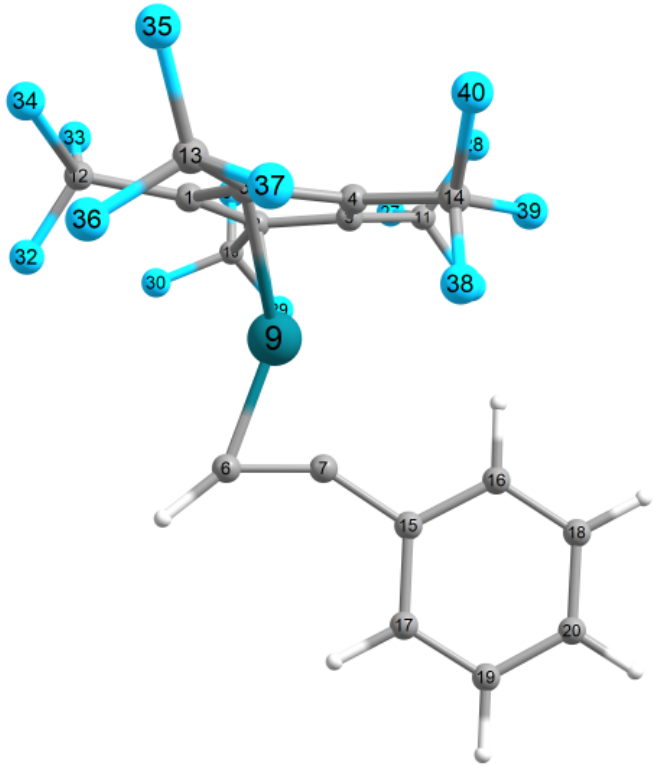

```
 Atom   29(F ):    -0.26786883
 Atom   30(F ):    -0.25069786
 Atom   31(F ):    -0.27215517
 Atom   32(F ):    -0.26288537
 Atom   33(F ):    -0.27807358
 Atom   34(F ):    -0.27164439
 Atom   35(F ):    -0.27991334
 Atom   36(F ):    -0.27334803
 Atom   37(F ):    -0.25649042
 Atom   38(F ):    -0.27284230
 Atom   39(F ):    -0.26086866
 Atom   40(F ):    -0.27937564
```

Atomic dipole-corrected Hirshfeld atomic charge (ADCH) for AC_RhCp^{SiF_3}

```
Final atomic charges, after normalization to actual number of
electrons
 Atom    1(C ):    -0.35313239
 Atom    2(C ):    -0.13220718
 Atom    3(C ):     0.19501965
 Atom    4(C ):    -0.84032912
 Atom    5(C ):    -0.07522728
 Atom    6(C ):    -1.46045674
 Atom    7(C ):     0.84826721
 Atom    8(H ):     1.28069123
 Atom    9(Rh):     1.64500754
 Atom   10(Si):     1.25811957
 Atom   11(Si):     1.32929231
 Atom   12(Si):     1.17954149
 Atom   13(Si):     1.28447158
 Atom   14(Si):     1.20407883
 Atom   15(C ):    -0.53758875
 Atom   16(C ):     0.70513605
 Atom   17(C ):     0.61878764
 Atom   18(C ):    -0.94924133
 Atom   19(C ):    -0.92372217
 Atom   20(C ):    -1.15758003
 Atom   21(H ):     0.05809190
 Atom   22(H ):     0.18556411
 Atom   23(H ):     0.06504828
 Atom   24(H ):     0.06129194
 Atom   25(H ):     0.08049813
 Atom   26(F ):    -0.40355626
 Atom   27(F ):    -0.36530624
 Atom   28(F ):    -0.36693336
 Atom   29(F ):    -0.41306342
 Atom   30(F ):    -0.36333085
 Atom   31(F ):    -0.34336268
 Atom   32(F ):    -0.42068629
 Atom   33(F ):    -0.32786223
 Atom   34(F ):    -0.35400407
 Atom   35(F ):    -0.35378350
 Atom   36(F ):    -0.40813818
 Atom   37(F ):    -0.35965292 Atom   39(F ):    -0.35284642
 Atom   38(F ):    -0.37142292 Atom   40(F ):    -0.36547312
```

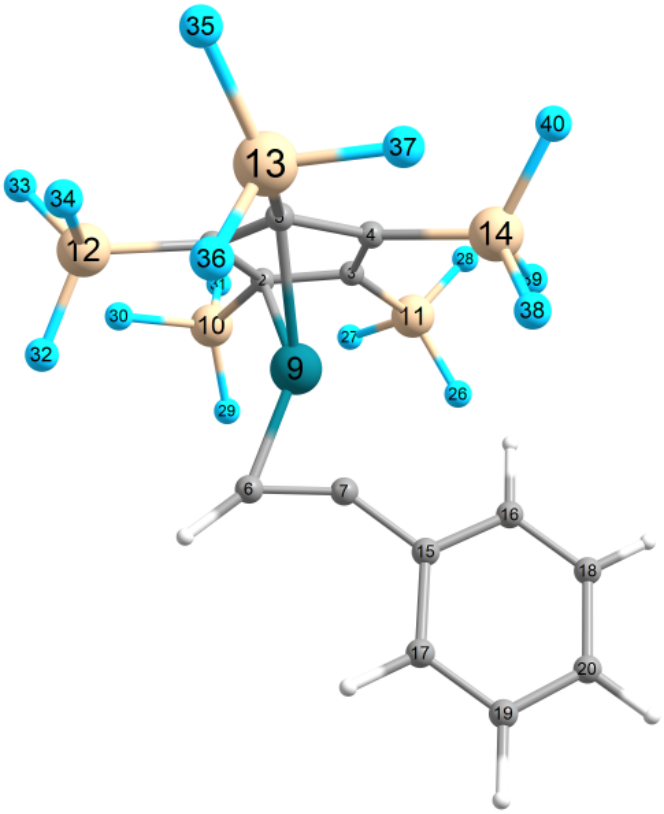

Atomic dipole-corrected Hirshfeld atomic charge (ADCH) for AC_RhCp^{CCl_3}

```
Final atomic charges, after normalization to actual number of
electrons
 Atom    1(C ):     0.03431694
 Atom    2(C ):     0.01527646
 Atom    3(C ):     0.80204182
 Atom    4(C ):    -0.05960440
 Atom    5(C ):     0.04845414
 Atom    6(C ):    -2.45778773
 Atom    7(C ):    -0.56517972
 Atom    8(H ):     1.18511203
 Atom    9(Rh):     0.73297537
 Atom   10(C ):     0.40824468
 Atom   11(C ):     0.52544225
 Atom   12(C ):     0.48182525
 Atom   13(C ):     0.49261240
 Atom   14(C ):     0.43631702
 Atom   15(C ):     0.19132315
 Atom   16(C ):    -0.00172925
 Atom   17(C ):    -0.05804412
 Atom   18(C ):    -0.20868048
 Atom   19(C ):    -0.12528259
 Atom   20(C ):    -0.08002211
 Atom   21(H ):     0.11597193
 Atom   22(H ):     0.11388689
 Atom   23(H ):     0.11151300
 Atom   24(H ):     0.12332566
 Atom   25(H ):     0.12622935
 Atom   26(Cl):    -0.15408524
 Atom   27(Cl):    -0.16584706
 Atom   28(Cl):    -0.15962244
 Atom   29(Cl):    -0.16149946
 Atom   30(Cl):    -0.16899776
 Atom   31(Cl):    -0.14593820
 Atom   32(Cl):    -0.14906091
 Atom   33(Cl):    -0.15783611
 Atom   34(Cl):    -0.16848856
 Atom   35(Cl):    -0.17375217
 Atom   36(Cl):    -0.15071426
 Atom   37(Cl):    -0.15327763
 Atom   38(Cl):    -0.17673628
 Atom   39(Cl):    -0.14233260
 Atom   40(Cl):    -0.16034925
```

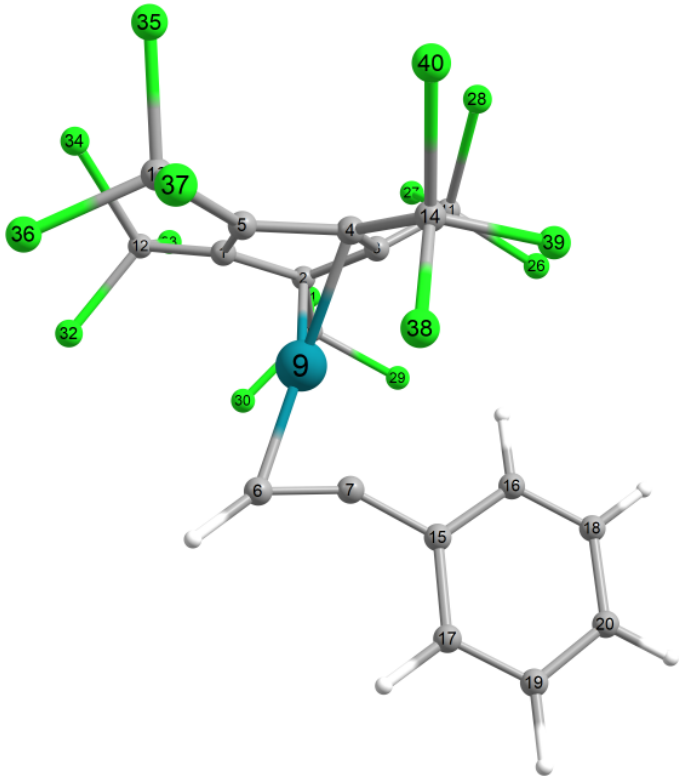

Atomic dipole-corrected Hirshfeld atomic charge (ADCH) for AC_RhCp^{CCl_3}

```
Final atomic charges, after normalization to actual number of
electrons
Atom    1(C ):    -0.05389813
 Atom    2(C ):     0.11102669
 Atom    3(C ):     0.10987707
 Atom    4(C ):    -0.02300907
 Atom    5(C ):    -0.71596812
 Atom    6(C ):     0.89008089
 Atom    7(C ):     0.47634172
 Atom    8(H ):     0.00372840
```

Atom	9(Rh):	-0.62678539
Atom	10(C):	-0.74520140
Atom	11(C):	-0.07931828
Atom	12(C):	-0.23111499
Atom	13(C):	-0.10759316
Atom	14(C):	-0.08661500
Atom	15(C):	0.77326173
Atom	16(H):	0.03637897
Atom	17(H):	0.13792285
Atom	18(H):	0.11098251
Atom	19(H):	0.10919829
Atom	20(H):	0.16584611
Atom	21(S):	1.92921375
Atom	22(O):	-0.64236778
Atom	23(O):	-0.92974581
Atom	24(S):	1.84771787
Atom	25(O):	-0.90675447
Atom	26(O):	-0.62233000
Atom	27(S):	1.91285154
Atom	28(O):	-0.93126210
Atom	29(O):	-0.90583952
Atom	30(S):	1.93615317
Atom	31(O):	-0.94422224
Atom	32(O):	-0.91883949
Atom	33(S):	1.92095347
Atom	34(O):	-0.63104418
Atom	35(O):	-0.93029403
Atom	36(O):	-0.62635723
Atom	37(O):	-0.62490680
Atom	38(O):	-0.90247394
Atom	39(O):	-0.89645793
Atom	40(O):	-0.93256657
Atom	41(H):	0.51616831
Atom	42(H):	0.50444725
Atom	43(H):	0.51169596
Atom	44(H):	0.50248198
Atom	45(H):	0.50863709